

CHARACTERISTICS OF SAR BACKSCATTERED INTENSITY AND ITS APPLICATION TO EARTHQUAKE DAMAGE DETECTION

FUMIO YAMAZAKI¹, WEN LIU² and HISAMITSU INOUE³

¹*Graduate School of Engineering, Chiba University, Japan.*

E-mail: fumio.yamazaki@faculty.chiba-u.jp

²*Graduate School of Engineering, Chiba University, Japan.*

E-mail: wen_liu@graduate.chiba-u.jp

³*Former Student, Chiba University, Japan.*

SAR images obtained before and after a natural disaster are considered to be useful for emergency response due to its all-weather and sunlight-independent characteristics. Recently, the spatial resolutions of SAR systems have been improved significantly. In this paper, SAR intensity images acquired before and after the 2008 Iwate-Miyagi, Japan, earthquake from ALOS/PALSAR (L-band) and TerraSAR-X (X-band) are employed to investigate the radar backscattering characteristics for various acquisition and surface conditions. The spatial resolution, radar frequency, flight path, and incidence angle were shown to affect SAR backscattering echo, depending on surface materials and roughness. Since the spatial resolution of TerraSAR-X is much higher than that of PALSAR, more detailed surface condition could be seen from the TerraSAR-X images. It is also observed that the difference of the backscattering coefficients at the pre- and post-event times gets large and their correlation coefficient becomes small at the locations of landslides and slope failures.

Keywords: Slope failure, landslide, SAR, backscatter, PALSAR, TerraSAR-X, the 2008 Iwate-Miyagi earthquake.

1 Introduction

Synthetic aperture radar (SAR) has the remarkable ability to examine the Earth's surface, regardless of weather or sunlight condition. The backscattering coefficient derived from SAR intensity images acquired before and after natural disasters have been used to extract changes/damages caused by the events (e.g., Yonezawa and Takeuchi 2001, Matsuoka and Yamazaki 2004, 2005).

Recently, the spatial resolutions of satellite SAR systems have been improved significantly; e.g. ALOS/PALSAR (Japan Aerospace Exploration Agency 2010; L-band, 10 m resolution in Fine mode) and TerraSAR-X (German Aerospace Center (DLR) 2010; X-band, 1 m resolution in Spot-Light mode). Hence, the change detection based on SAR

intensity images will be more promising to draw damage distributions.

In this paper, high-resolution satellite SAR intensity images acquired before and after the 2008 Iwate-Miyagi, Japan, earthquake are employed to investigate the radar backscattering characteristics for various acquisition and surface conditions and to extract the damage areas caused by the event.

2 The 2008 Iwate-Miyagi Earthquake and Satellite SAR Images

A magnitude 7.2 (M_J) earthquake hit an inland region near the border of Iwate and Miyagi prefectures in the northern Japan on June 14, 2008. Since the epicenter is located in a mountainous region, the most roads in the affected areas were blocked by slope failures and landslides, and many villages were

isolated. Hence, airborne and satellite remote sensing technologies were employed to obtain damage distribution in this event (Geographical Survey Institute of Japan 2008).

As one of versatile satellites, ALOS (The Advanced Land Observing Satellite) captured the affected areas by its PALSAR sensor both from the ascending and descending paths (Fig. 1). Both a pre-event image (2008/3/23) and a post-event image (2008/6/23) were obtained from the ascending path (nighttime) and only a post-event image (2008/7/16) was obtained from the descending path (daytime) as shown in Fig. 2. These images were captured by high-resolution (FBS) mode (6.25m/pixel) with incidence angle 34.3 degrees.

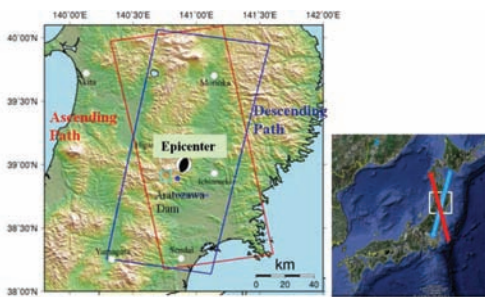


Fig. 1 Observed areas of ALOS/PALSAR from the ascending and descending paths for the 2008 Iwate-Miyagi, Japan, earthquake.

Figure 3 compares the SAR intensity images from the ascending and descending paths in Aratozawa Dam area, where a large-scale landslide occurred in the upstream of the dam lake. In the ascending path, the radar beam illuminates the earth surface obliquely from west to east, and hence at the top of the landslide, radar shadow was observed. On the contrary, the landslide cliff looks “brightest” from the descending path because the cliff is almost a right angle to the radar beam. Clear

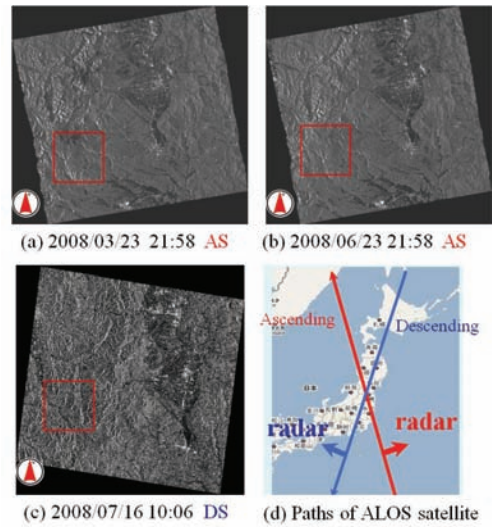


Fig. 2 PALSAR images of the affected area of the 2008 Iwate-Miyagi earthquake. Red squares correspond to the area of TerraSAR-X images in Fig. 4.

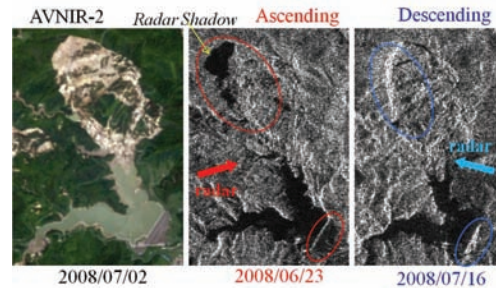
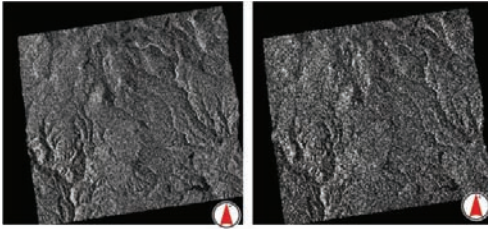


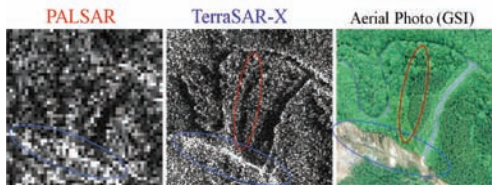
Fig. 3 Comparison of PALSAR images from the ascending and descending paths in Aratozawa Dam area.

differences between the two images are also seen at the embankment of the dam and the bottom edge of the large landslide.

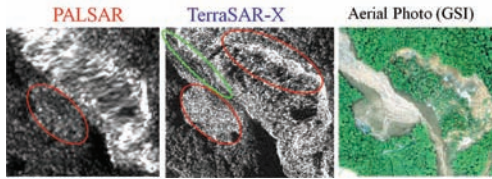
TerraSAR-X also observed the affected areas (Midorikawa and Miura, 2009) at three time instants after the earthquake by high-resolution SpotLight mode (0.75m/pixel) with incidence angle 49.3 degrees. Figure 4 compares the high-resolution SAR images acquired two days after the earthquake (2008/06/16) and 1.5 months after (2008/07/30). Since all the other acquisition



(a) 2008/06/16 17:37 (b) 2008/07/30 17:37
 Fig. 4 TerraSAR-X images of the affected area acquired after the earthquake by SpotLight mode from the ascending path with incidence angle 49.3 degree.



(a) The north of the landslide at Aratozawa dam



(b) Debris flow and landslide at Komanoyu Spa

Fig. 5 Comparison of the post-event PALSAR and TerraSAR-X images from the ascending path for two locations.

conditions are the same, the difference of the two images corresponds to the change or the progress of damage in this period.

These SAR intensity images were investigated from the viewpoint of microwave frequency (L-band or X-band) and spatial resolution. Since the study area is mountainous and topographic effects are significant, we used orthorectified products of these SAR images. Figure 5 compares the post-event SAR images for the same area. For the scene at the upstream of Aratozawa Dam, TerraSAR-X provides much finer texture, due to the difference of resolution. A narrow path and small valley in the forest can be identified as radar shadow. From the images at

Komanoyu Spa, the river bed covered by debris flow looks much brighter for TerraSAR-X than for PALSAR. This difference may be due to the difference of the radar wavelength.

3 Change Detection Using PALSAR Images

ALOS/PALSAR images of the affected areas were acquired both before (2008/3/23) and after (2008/6/23) the earthquake with the same radar conditions (L-band, HH polarization, ascending path, FBS mode, off-nadir angle 34.3 degrees, ground-resolution 6.25 m).

To detect changes due to a natural disaster, Matsuoka and Yamazaki (2004, 2005) have used multi-looked intensity images taken before and after an earthquake. It is desirable that the acquisition dates are close, as much as possible, to the earthquake occurrence day and the both observation conditions are similar. After co-registration for the pre- and post-event images, each image was filtered using a Lee filter (Lee 1980) with 10 x 10 pixel window to reduce speckle noise. The difference of the backscattering coefficients, d [dB], in Eq. (1) and the correlation coefficient, r , in Eq. (2), were derived from the two filtered images.

$$d = 10 \cdot \log_{10} \bar{I}a_i - 10 \cdot \log_{10} \bar{I}b_i \quad (1)$$

$$r = \frac{N \sum_{i=1}^N I a_i I b_i - \sum_{i=1}^N I a_i \sum_{i=1}^N I b_i}{\sqrt{\left(N \sum_{i=1}^N I a_i^2 - \left(\sum_{i=1}^N I a_i \right)^2 \right) \cdot \left(N \sum_{i=1}^N I b_i^2 - \left(\sum_{i=1}^N I b_i \right)^2 \right)}} \quad (2)$$

where i is the pixel number, $I a_i$ and $I b_i$ are the digital numbers of the post- and pre-event

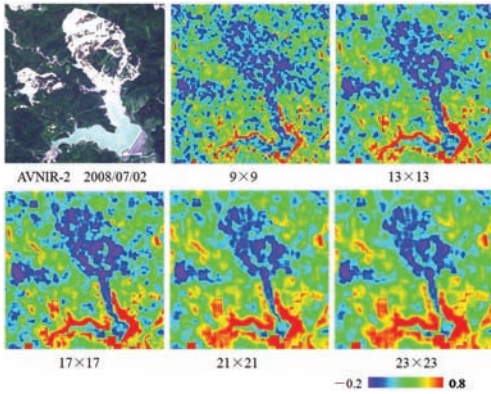


Fig. 6 Comparison of the window size for PALSAR to obtain the correlation coefficient.

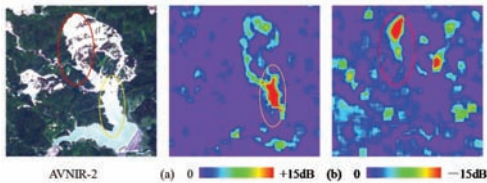


Fig. 7 The difference of the post- and pre-event backscattering coefficients for PALSAR images, highlighting positive values (a) and negative values (b).

images, $\bar{I}a_i$ and $\bar{I}b_i$ are the corresponding averaged values over the $N (=k^2)$ pixels window surrounding the i -th pixel.

Figure 6 compares the effect of window size (N) for PALSAR data on calculating the correlation coefficient by Eq. (2). For the SAR data pair around Aratozawa Dam, low correlation areas become almost coincidental with large landslide zones and the dam lake by increasing the window size. High correlation areas are seen in the surroundings of the lake and the dam, probably due to high contrast in backscattering coefficients between water and land. Based on this kind of examination, the window size for PALSAR was determined as 21x21 in this study.

The difference of the post-event and pre-event backscattering coefficients by eq. (1) is plotted in Fig. 7 for the same area. In the

figure, a part of the dam lake filled by the large landslide shows a high positive value, due to increase of the backscattering coefficient. The large negative difference is seen in the post-event radar shadow (landslide cliff) areas. The difference plot, like this, is also a good indicator of affected areas. But we need to know the original surface condition and topography to explain the changes due to an earthquake.

4 Change Detection Using TerraSAR-X Images

For the two TerraSAR-X images obtained at the two post-event times (2008/6/16 and 2008/7/30), a Lee filter with 21 x 21 pixel window was applied to reduce speckle noise. Then the difference of the backscattering coefficients and the correlation coefficient for the two images were calculated as shown in Fig. 8. In the figure, low correlation is seen in the dam lake and the radar shadows although the both images were acquired in the post-event period. The water body presents low correlation, especially for X-band microwaves, due to water-surface undulation by wind. The landslide cliff shows low correlation because of low intensity values in the area, in spite of no much surface change in this period. Relatively large increases of backscattered coefficients are seen in the rim of the large landslide probably due to the progress of the displacement, and in the lake boundary, due to the reduction of water level.

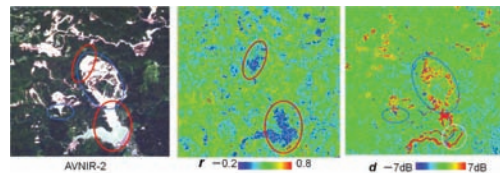


Fig. 8 The correlation coefficient, r , and the difference of the backscattering coefficients, d , for the two post-event TerraSAR-X images around Aratozawa Dam.

5 Conclusions

Using PALSAR and TerraSAR-X intensity images obtained before and after the 2008 Iwate-Miyagi, Japan earthquake, the extraction of changes associate with the earthquake, e.g. slope failures, landslides, reduction of the dam lake, was carried out. First, the resolution, radar frequency, flight path, and incidence angle of microwaves were shown to affect SAR backscattering echo, depending on surface materials and roughness. Comparing the backscattering coefficients obtained for two different time instants, the correlation coefficient was seen to get small for heavily impacted surfaces. The difference of backscattering coefficients was also seen to get large for significant changes in surface roughness and elevation.

Acknowledgments

The TerraSAR-X images used in this study were made available from SAR Application Research Committee, organized by PASCO Corporation, Tokyo, Japan.

References

- DLR, http://www.dlr.de/eo/en/desktopdefault.aspx/tabid-5725/9296_read-15979/, 2010.
- Geographical Survey Institute of Japan, <http://cais.gsi.go.jp/Research/topics/topic080625/index.html>, 2008.
- Japan Aerospace Exploration Agency, <http://www.eorc.jaxa.jp/ALOS/en/index.htm>, 2010.
- Lee, J.S., Digital image enhancement and noise filtering by use of local statistics, *IEEE Trans. Pattern Analysis and Machine Intelligence*, 2(2), 165-168, 1980.
- Matsuoka, M. and Yamazaki, F., Use of Satellite SAR Intensity Imagery for Detecting Building Areas Damaged due to Earthquakes, *Earthquake Spectra*, 20(3), 975-994, 2004.
- Matsuoka, M. and Yamazaki, F., Building damage mapping of Iran earthquake using Envisat/ASAR intensity imagery, *Earthquake Spectra*, 21(S1), S285-S294, 2005.
- Midorikawa, s. and Miura, H., Damage and High-Resolution SAR Image in the 2008 Iwate-Miyagi-Nairiku, Japan Earthquake, *6th International Workshop on Remote Sensing for Disaster Applications*, Pavia, Italy, 2008.
- Yonezawa, C. and Takeuchi, S, Decorrelation of SAR Data by Urban Damages Caused by the 1995 Hyogoken-nanbu Earthquake, *International Journal of Remote Sensing*, 22(8), 1585-1600, 2001.